Force Spectroscopy of the Leukocyte Function-Associated Antigen-1/Intercellular Adhesion Molecule-1 Interaction

Xiaohui Zhang, Ewa Wojcikiewicz, and Vincent T. Moy
Department of Physiology and Biophysics, University of Miami School of Medicine, Miami, Florida 33136 USA

ABSTRACT Interactions between leukocyte function-associated antigen-1 (LFA-1) with its cognate ligand, intercellular adhesion molecule-1 (ICAM-1) play a crucial role in leukocyte adhesion. Because the cell and its adhesive components are subject to external perturbation from the surrounding flow of blood, it is important to understand the binding properties of the LFA-1/ICAM-1 interaction in both steady state and in the presence of an external pulling force. Here we report on atomic force microscopy (AFM) measurements of the unbinding of LFA-1 from ICAM-1. The single molecule measurements revealed the energy landscape corresponding to the dissociation of the LFA-1/ICAM-1 complex and provided the basis for defining the energetic determinants of the complex at equilibrium and under the influence of an external force. The AFM force measurements were performed in an experimental system consisting of an LFA-1-expressing T cell hybridoma, 3A9, attached to the end of the AFM cantilever and an apposing surface expressing ICAM-1. In measurements covering three orders of magnitude change in force loading rate, the LFA-1/ICAM-1 force spectrum (i.e., unbinding force versus loading rate) revealed a fast and a slow loading regime that characterized a steep inner activation barrier and a wide outer activation barrier, respectively. The addition of Mg^{2+}, a cofactor that stabilizes the LFA-1/ICAM-1 interaction, elevated the unbinding force of the complex in the slow loading regime. In contrast, the presence of EDTA suppressed the inner barrier of the LFA-1/ICAM-1 complex. These results suggest that the equilibrium dissociation constant of the LFA-1/ICAM-1 interaction is regulated by the energetics of the outer activation barrier of the complex, while the ability of the complex to resist a pulling force is determined by the divalent cation-dependent inner activation barrier.

INTRODUCTION

Integrins are $\alpha\beta$ heterodimeric transmembrane adhesion molecules, constitutively expressed in a wide variety of cells (Hynes, 1992). They mediate cell adhesion by binding to components of the extracellular matrix or to another cell by binding to members of the immunoglobulin (Ig) superfamily (Springer, 1990). In the early 1980s, leukocyte function-associated antigen-1 (LFA-1; CD11a/CD18, $\alpha_L\beta_2$) was identified as the predominant integrin in leukocytes (Sanchez-Madrid et al., 1983). The major ligand of LFA-1 in intercellular adhesion is intercellular adhesion molecule-1 (ICAM-1; CD54), a cell surface glycoprotein consisting of five extracellular Ig-like domains (Marlin and Springer, 1987; Siu et al., 1989; Staunton et al., 1990). The LFA-1/ICAM-1 interaction modulates several important lymphocyte functions, including antigen presentation, lymphocyte extravasation, and cell migration (Dustin and Springer, 1991; Springer, 1994).

The ICAM-1 binding site of LFA-1 has been localized to an inserted domain, the α_L I domain, that projects from the N-terminal seven-bladed β-propeller domain of the α chain (Larson et al., 1989; Springer, 1997). More specifically, the predicted binding surface centered on a metal ion-dependent adhesion site (MIDAS) motif of the α_L I domain (Lee et al., 1995). A divalent cation (i.e., Mg^{2+}) facilitates ICAM-1 binding by coordinating with five amino acids of the MIDAS and glutamate 34 in the first Ig domain of ICAM-1 (Stanley and Hogg, 1998). The complete binding surface covers an area of over 100 $Å^2$ that includes essential hydrophilic and hydrophobic amino acid residues (Bella et al., 1998; Edwards et al., 1998; Huang and Springer, 1995; Qu and Leahy, 1995).

Like most integrins, LFA-1 is expressed on the cell surface in one of two affinity states (Diamond and Springer, 1994). Resting leukocytes express a form of LFA-1 that binds to ICAM-1 with low affinity. Depending on the cell type, LFA-1 is activated by different external signals. For T lymphocytes, engagement of the T cell receptor results in a cascade of intracellular processes that augment the affinity of LFA-1 for ICAM-1 (Stewart et al., 1996). Changes in the affinity state of LFA-1 can be artificially induced by extracellular Mg^{2+} or Mn^{2+} (Ganpule et al., 1997; Stewart et al., 1996). The activation of LFA-1 by Mg^{2+} or Mn^{2+} appears to be a complex process that is initiated by the binding of the divalent cation to the MIDAS of the βI domain, followed by the transduction of signal across the interchain junction to the β-propeller domain, which subsequently induces the α_L I domain to expose its high-affinity binding site for ICAM-1 (Lu et al., 2001).

The interaction between LFA-1 and ICAM-1 has been characterized by measurements of its association rate, dissociation rate, and equilibrium binding affinity (Lollo et al., 1993; Lupher et al., 2001; Tominaga et al., 1998; Woska et al., 1996). Estimates of the equilibrium dissociation constant, K_d, for the low and high-affinity LFA-1/ICAM-1

Submitted april 3, 2002, and accepted for publication June 7, 2002.

Address reprint requests to Vincent T. Moy, Department of Physiology and Biophysics, University of Miami School of Medicine, 1600 N.W. 10th Avenue, Miami, FL 33136, Tel.: 305 243-3201; Fax: 305 243-5931; E-mail: vmoy@newssun.med.miami.edu.

0006-3495/02/10/2270/10 $2.00

interactions are 6.7×10^{-5} M and 3.6×10^{-7} M, respectively (Lollo et al., 1993). However, it is not well understood how a change in the binding affinity translates into changes in the mechanical strength of the LFA-1/ICAM-1 bond. Here, we report on the application of atomic force microscopy (AFM) (Binnig et al., 1986; Heinz and Hoh, 1999) to determine the effects of a pulling force on the off-rate of the LFA-1/ICAM-1 complex. Similar approaches, including the biomembrane force probe, have been used to study the unbinding of streptavidin-biotin complex, complementary strands of DNA, and other adhesion systems (Florin et al., 1994; Lee et al., 1994a, b; Merkel et al., 1999; Evans et al., 2001). These direct force measurements have provided the means to probe the dissociation pathway of the biomolecular complex (Willemsen et al., 2000).

MATERIALS AND METHODS

Cells

The 3A9 cell line, the ICAM-1-expressing fibroblast line, FT16.II, and the ICAM-1 deficient fibroblast cell line, FT16.6C5 (Kuhlman et al., 1991; Lollo et al., 1993) were maintained in continuous culture in RPMI 1640 medium supplemented with 10% heat-inactivated fetal calf serum (Irvine Scientific, Santa Ana, CA), penicillin (50 U/ml, Gibco BRL, Grand Island, NY), and streptomycin (50 μg/ml, GIBCO BRL), and were expanded on a 3-day cycle. The fibroblast cells were plated on a 35-mm tissue culture dish at ~10% confluency for measurements on the following day.

Attachment of cell to AFM cantilever

3A9 cells were attached to the AFM cantilever by concanavalin A (Con A)-mediated linkages (Fig. 1). To prepare the con A-functionalized cantilever, the cantilevers were soaked in acetone for 5 min, UV-irradiated for 30 min, and incubated in biotinamidocaproyl-labeled bovine serum albumin (biotin-BSA, 0.5 mg/ml in 100 mM $NaHCO_3$, pH 8.6; Sigma, St. Louis, MO) overnight at 37°C. The cantilevers were then rinsed three times with phosphate buffered saline (PBS, 10 mM PO_4^{3-}, 150 mM NaCl, pH 7.3) and incubated in streptavidin (0.5 mg/ml in PBS; Pierce, Rockford, IL) for 10 min at room temperature. Following the removal of unbound streptavidin, the cantilevers were incubated in biotinylated Con A (0.5 mg/ml in PBS; Sigma) and then rinsed with PBS. To attach the cell to the cantilever, the tip of the Con A-functionalized cantilever was positioned above the center of a cell and lowered onto the cell for ~1 s. To obtain an estimate of the strength of the cell-cantilever linkage, we allowed the attached cell to interact with a substrate coated with Con A for 1 min. Upon retraction of the cantilever, separation always ($N > 20$) occurred between the cell and the Con A-coated surface. The average force needed to induce separation was >2 nN. These measurements, thus, revealed that the linkages supporting cell attachment to the cantilever are >2 nN and much larger than the unbinding force of the individual LFA-1/ICAM-1 bond.

Immobilized ICAM-1

The center of a 35-mm tissue culture dish (Falcon 353001) was coated with a soluble truncated form of murine ICAM-1 (sICAM-1) (Kuhlman et al., 1991). sICAM-1 includes the first four extracellular immunoglobulin domains and a portion of the fifth domain of ICAM-1, but lacks the transmembrane and cytoplasmic domains. sICAM-1 at 50 μg/ml in PBS was physioadsorbed overnight at 4°C. Unbound sICAM-1 was removed and bovine albumin (Sigma) at 100 μg/ml in PBS was used to block the exposed surface of the dish.

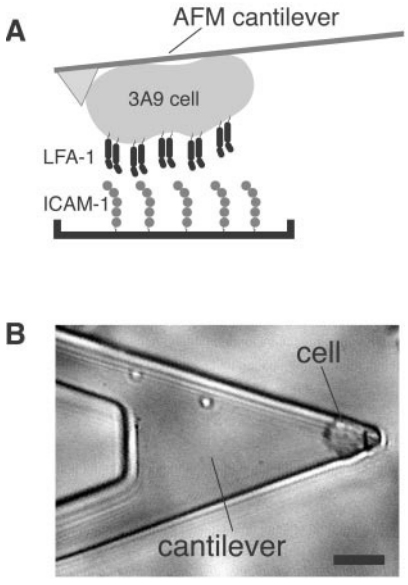

FIGURE 1 Schematic representation of our experimental system. (*A*) A T-cell attached to the end of an AFM cantilever is used to study its interaction with immobilized ICAM-1. A similar experimental design was used to measure the adhesive interactions between a T cell and ICAM-1 expressed on the surface of another cell. (*B*) Micrograph of a 3A9 cell attached to the end of an AFM cantilever. The bar is 20μm.

AFM force measurements

The AFM force measurements were performed on an apparatus designed to be operated in the force spectroscopy mode (Benoit et al., 2000; Heinz and Hoh, 1999; Willemsen et al., 2000). A 3A9 cell was attached to the end of the AFM cantilever as described above. A piezoelectric translator was used to lower the cantilever/cell onto the sample, either an ICAM-1 coated dish or a fibroblast cell. The interaction between the attached 3A9 cell and the sample was given by the deflection of the cantilever, which was measured by reflecting a laser beam off the cantilever into a position sensitive two segment photodiode detector. AFM cantilevers were purchased from TM Microscopes (Sunnyvale, CA). The largest triangular cantilever (320 μm long and 22 μm wide) from a set of five on the cantilever chip was used in our measurements. These cantilevers were calibrated by analysis of their thermally induced fluctuation to determine their spring constant (Hutter and Bechhoefer, 1993). The experimentally determined spring constants were consistent with the nominal value of 10 mN/m given by the manufacturer.

Measurements of unitary LFA-1/ICAM-1 unbinding forces were obtained under conditions that minimized contact between the 3A9 cell and the sample. An adhesion frequency of <30% in the force measurements ensured that there is a >85% probability that the adhesion event is mediated by a single LFA-1/ICAM-1 complex (Tees et al., 2001a). We were able to acquire measurements at loading rates (r_f) between 20 and 50,000 pN/s. This was achieved by varying the retraction rate of the cantilever (v) from 0.1 to 15 μm/s, and as a result of variations in the local compliance of the cell that allowed for the effective spring constant of the cell-cantilever combination (k_s) to have a range of values between 0.1 and 5 mN/m (i.e., $r_f = k_s \times v$). As shown in trace 2 of Fig. 3, both the system

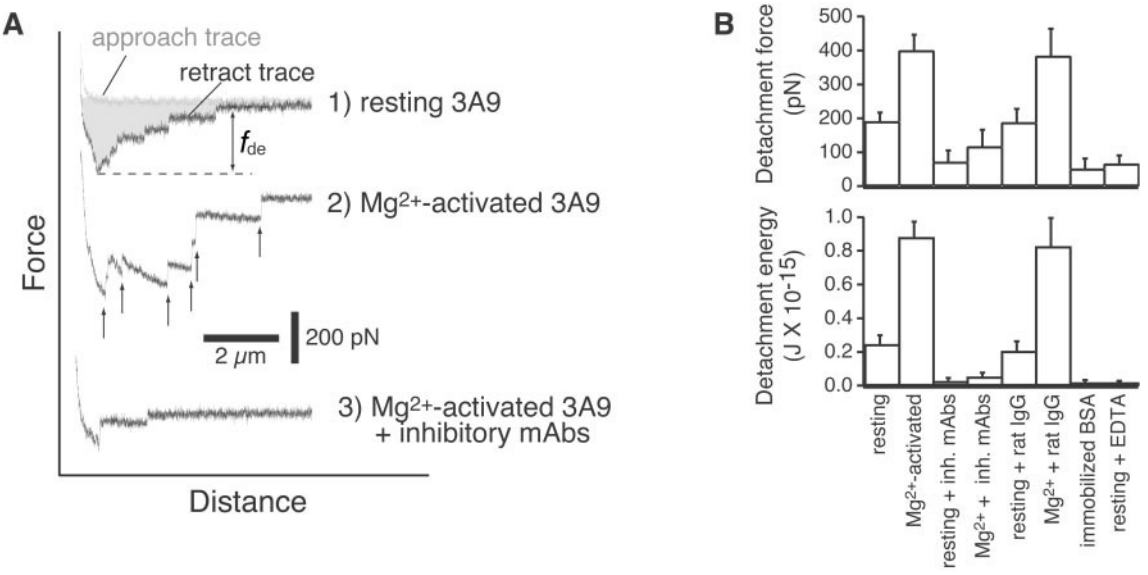

FIGURE 2 AFM force measurements of cell adhesion. (*A*) A series of AFM force-displacement traces between a 3A9 cell and iICAM-1 acquired under different conditions. For traces 2 and 3, the cell was treated with 5 mM $MgCl_2$ and 1 mM EGTA. Trace 3 was acquired in the presence of 50 μg/ml FD441.8 (anti-LFA-1 mAb) and 50 μg/ml BE29G1 (anti-ICAM-1 mAb). All traces were acquired with the same cell in the order listed. The shaded area in trace 1 corresponds to the work done to detach the cell from the ICAM-1 coated surface. f_{de} is the detachment force supported by the adhesive bonds formed between the cell and the substrate. The arrows in trace 2 point to positions in the trace where an LFA-1/ICAM-1 complex ruptured. All measurements were acquired using a cantilever retaction speed of 2 μm/s, a contact duration of 5s, and a compression force of 300 pN. (*B*) Detachment force and detachment energy of cell-substrate interaction under different conditions. The bar graphs summarize the results from six separate sets of measurements, with each series of measurements repeated once with a different cell. In the first set, force measurements were acquired measurements (>10/cell) from the resting cells. The same cells were stimulated with Mg^{2+}/EGTA to activate LFA-1, and a set of >10 measurements were collected. Subsequently, the same cells were treated with the inhibitory antibodies to demonstrate that the interaction between high-affinity LFA-1 and ICAM-1 can be blocked. To determine the effects of inhibitory antibodies, control polyclonal rat IgG antibodies and EDTA on the adhesion of resting cells to iICAM-1, a set of >10 force measurements were acquired from the resting cells in the absence of the test reagents to determine whether the resting cells adhered to ICAM-1 at the same baseline level. One of the test reagents (i.e., inhibitory antibodies, control polyclonal rat IgG antibodies, and EDTA) was subsequently added and a set of >10 measurements were recorded to determine the effects of the reagents on cell adhesion. To determine the effects of the inhibitory antibodies and polyclonal rat IgG antibodies on the adhesive properties of Mg^{2+}-activated cells, force measurements were first acquired from the resting cells. The cells were then stimulated with Mg^{2+}/EGTA. Subsequent measurements were made to confirm that the cells were activated before the addition of the inhibitory antibodies or polyclonal rat IgG. The substrate was coated with ICAM-1 except in one experiment, where bovine serum albumin (BSA) was used as a negative control. The concentrations of $MgCl_2$ and antibodies used in this set of measurements are the same as in (*A*). The error bars are the standard deviation from a set of >20 measurements from two cells.

spring constant, k_s, and the unbinding force of the LFA-1/ICAM-1 complex, f_u, were simultaneously acquired in one measurement.

At fast cantilever retraction speeds (>1μm/s), the hydrodynamic drag on the cantilever resulted in smaller forces recorded than were actually applied to rupture the LFA-1/ICAM-1 complex (Evans et al., 2001). To correct for the hydrodynamic force exerted on the cantilever, we determined the damping coefficient of the cantilever ξ (~2 pN-s/μm) in the culture medium. The unbinding force plotted in Figs. 3–6 is the sum of the measured force and the hydrodynamic force. All AFM force measurements were carried out at 25°C with fresh culture medium supplemented with 10 mM HEPES buffer.

RESULTS

Adhesion of 3A9 cells to immobilized ICAM-1 measured by AFM

The AFM was used to measure the adhesive interaction between cells expressing LFA-1 and immobilized ICAM-1 (iICAM-1). The cell adhesion measurements were carried out with an LFA-1 expressing murine T-cell hybridoma (i.e., 3A9) coupled to the AFM cantilever and a soluble form of ICAM-1 that was adsorbed to the surface of a tissue culture dish (see Fig. 1). The 3A9 cell was lowered onto the dish to initiate the binding of LFA-1 to ICAM-1. Following surface contact, the interaction between the cell and the ICAM-1-coated surface was regulated by the applied force of the cantilever that pressed the cell against the the dish. After a specified contact duration, the 3A9 cell was withdrawn from the dish surface at a predetermined separation rate while the force versus piezo displacement trace of the detachment process was recorded. Fig. 2 *A* presents a series of AFM force versus distance traces acquired between 3A9 cells and iICAM-1 under different experimental conditions. In these measurements, the LFA-1/ICAM-1 interactions were detected by the downward deflections of the cantilever during cantilever retraction. A typical measurement involved the formation of multiple LFA-1/ICAM-1 com-

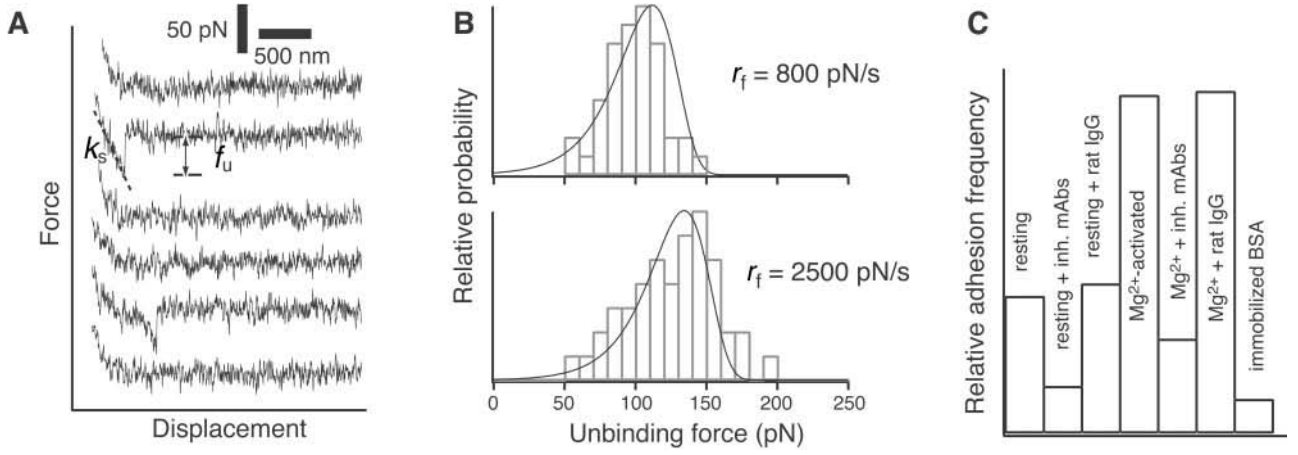

FIGURE 3 (*A*) Force-displacement (retract) traces between 3A9 and iICAM-1 under conditions of minimal contact. Two of the six traces (2nd and 5th) revealed adhesion. f_u is the unbinding force of the LFA-1/ICAM-1 bond. k_s is the system spring constant and was derived from the slope of the force-displacement trace. The cantilever retraction rate of the measurements was 2 μm/s. (*B*) Force distributions of the interaction between a Mg^{2+}-activated 3A9 cell and iICAM-1 acquired at loading rates of 800 pN/s (*upper histogram*) and 2500 pN/s (*lower histogram*). The fitted curves were obtained using Eq. 1 and the Bell model parameters listed in Table 1. (*C*) Relative frequency of adhesion between 3A9 cells and iICAM-1 under different conditions with minimal contact.

plexes that did not necessarily rupture simultaneously during surface separation. The "sawtooth" profile observed in the AFM traces suggests that these complexes often ruptured sequentially before final separation, with each sharp transition in the retraction trace interpreted as a breakage of one or more LFA-1/ICAM-1 complexes (Fig. 2 *A*).

The mechanical work (i.e., detachment energy) and the force required to detach the cell are quantitative measures of cell adhesion. An estimate of the detachment energy was derived from integrating the adhesive force over the displacement of the cantilever. In terms of both detachment energy and detachment force, 3A9 cells, stimulated with 5 mM $MgCl_2$ and 1 mM EGTA, adhered more tightly to ICAM-1 than resting cells (Fig. 2 *B*). These results are consistent with results reported by others using conventional cell adhesion assays (Ganpule et al., 1997; Stewart and Hogg, 1996). Our measurements also revealed that cell adhesion was inhibited by FD411.8 and BE29G1, monoclonal antibodies against LFA-1 and ICAM-1, respectively, and by 5 mM EDTA, but not by polyclonal rat IgG antibodies (Fig. 2 *B*). The adhesion of 3A9 cells to immobilized bovine albumin was negligible. Together, these results demonstrate that measured adhesion is mediated by the specific interaction between LFA-1 and ICAM-1. It should be noted that detachment energy measured here is the work done to rupture the LFA-1/ICAM-1 complexes and to stretch the cell during cell separation. Hence, an increase in detachment energy may reflect changes in bond strength, bond number, and/or cell compliance. A goal of the current study is to determine the effects of cell activation on the bond strength of the LFA-1/ICAM-1 complex.

Single molecule measurements of the forced unbinding of the LFA-1/ICAM-1 complex

To assess the bond strength of the individual LFA-1/ICAM-1 complex, contact between the 3A9 cell and iICAM-1 was minimized by reducing both contact duration (~50 ms) and compression force. Examples of measurements acquired under these conditions are given in Fig. 3 *A*. In contrast to the measurements presented in Fig. 2 *A,* these measurements frequently revealed no adhesion. When adhesion did take place, the AFM force-displacement trace revealed a linear increase in force, followed by a single sharp transition that signaled the breakage of a single LFA-1/ICAM-1 complex. The observed linear force profile in the majority of measurements is consistent with force measurements acquired in other cell systems (Benoit et al., 2000), but differed from the nonlinear response observed in the extension of molecular springs and unfolding of proteins such as titin (Oberhauser et al., 1998; Rief et al., 1997a, b). The unbinding force of the individual LFA-1/ICAM-1 complex was derived from the magnitude of the force transition with corrections for hydrodynamic drag. Fig. 3 *B* summarizes the force distribution for unbinding of the LFA-1/ICAM-1 complex at two different loading rates. In general, the force distribution is shifted toward higher values with increasing loading rates, an observation that is consistent with the dynamic response of other ligand-receptor systems (Evans et al., 2001; Merkel et al., 1999; Tees et al., 2001a).

Due to the high sensitivity of AFM measurements, it is conceivable that not all of the measurements stemmed from the LFA-1/ICAM-1 interaction. Without a defining signature or an independent method for identifying the protein of interest, it is not possible to know definitively the origin of

a given force measurement. In cases like these, the specificity of the molecular interaction is confirmed by examining the frequency of adhesion in test and control experiments (Evans et al., 2001; Tees et al., 2001a). Under identical experimental conditions, we noted that the frequency of cell adhesion to iICAM-1 is higher when the cells were stimulated with Mg^{2+}/EGTA, reflecting changes toward a higher affinity state of LFA-1 (Fig. 3 *C*). In contrast, the addition of monoclonal antibodies against either LFA-1 or ICAM-1 significantly lowered the frequency of adhesion of both resting and activated cells, while the addition of polyclonal rat IgG did not change the frequency of adhesion. Moreover, both resting and stimulated 3A9 cells exhibited lower frequency of adhesion to immobilized bovine albumin than to iICAM-1. These experiments demonstrate that the adhesion between the 3A9 cell and iICAM-1 can be attributed to the interaction between LFA-1 and ICAM-1 in a vast majority of the force measurements.

Dynamic strength of individual LFA-1/ICAM-1 complexes

As shown in Fig. 4, the average unbinding force of the LFA-1/ICAM-1 complex increases over three orders of magnitude change in loading rate. Moreover, two loading regimes in the LFA-1/ICAM-1 interactions were evident in the force spectrum (plot of unbinding force versus loading rate). There was a gradual increase in unbinding force with increasing loading rate up to ~10,000 pN/s. Beyond this point, there was a second loading regime that exhibited a faster increase in unbinding force. Induction of high-affinity LFA-1 by Mg^{2+}/EGTA resulted in higher LFA-1/ICAM-1 unbinding forces that were pronounced in the slow loading regime (Fig. 4 *A*). Interestingly, there was no significant difference in dynamic response of the low and high-affinity complexes in the fast loading regime (i.e., loading rates >10,000 pN/s). The dynamic response of the LFA-1/ICAM-1 complex in the fast-loading regime appears to be divalent cation-dependent, as the unbinding force acquired in this region of the spectra was suppressed by the addition of 5 mM EDTA (Fig. 4 *B*). The high-affinity state of LFA-1 was also induced by the addition of 1 mM Mn^{2+}, but not by 5 mM Ca^{2+} (data not shown).

Force measurements were also carried out between 3A9 cells and FT16.11, a fibroblast cell line that expressed the wild-type membrane bound form of ICAM-1. To demonstrate that it is possible to detect a single LFA-1/ICAM-1 interaction in this system, we confirmed that the 3A9 cells adhered to the FT16.I1 at a higher frequency than to the ICAM-1 negative fibroblast cell line, FT16.6C5. Moreover, as shown in Fig. 5 *A,* the measured nonspecific forces between 3A9 and FT16.6C5 were smaller than the LFA-1/ICAM-1 unbinding forces acquired from the interaction between 3A9 and FT16.I1. Because FT16.6C5 and FT16.I1 differed only in their expression of ICAM-1, we attribute

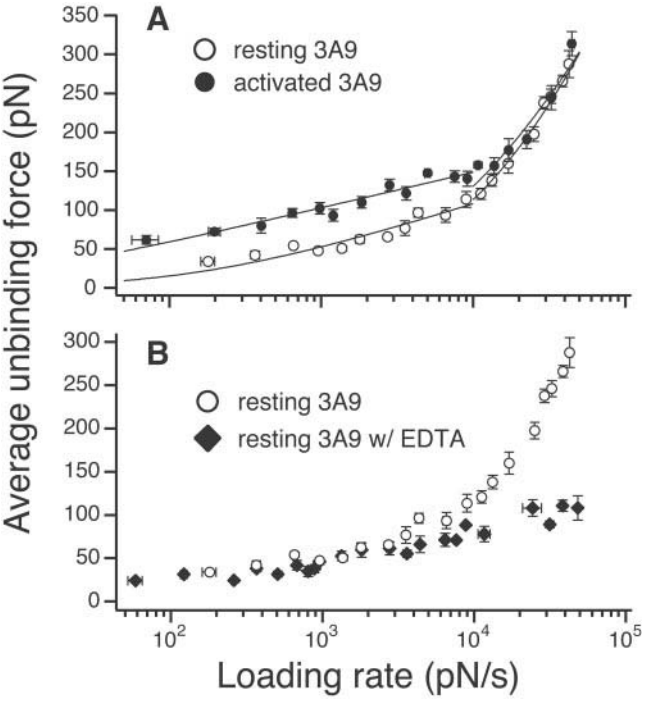

FIGURE 4 Measurements of individual LFA-1/ICAM-1 unbinding forces between 3A9 cells and iICAM-1 as a function of loading rate. (*A*) Measurements between iICAM-1 and resting 3A9 cells (*open circles*) or Mg^{2+}/EGTA-activated cell (filled circles). The fitted curves were derived from fitting Eq. 2 to the data. (*B*) Measurements between resting 3A9 cells and ICAM-1 in the absence (circles) or presence (*diamonds*) of 5 mM EDTA. The specificity of the LFA-1/ICAM-1 interaction in the presence of EDTA was confirmed by antibody inhibition. Under identical experimental conditions, the frequency of adhesion was reduced by >50% following addition of mAb FD441.8 (50 μg/ml) and mAb BE29G1 (50 μg/ml). Each of the force spectra were acquired using five cells with an average of 100 measurements/cell. The error bars are the standard error of the measurements.

the difference in adhesive properties between these two cell lines to the interaction of LFA-1 and ICAM-1. In general, the measurements acquired between opposing 3A9 and FT16.I1 cells were nearly identical to the measurements that we obtained using iICAM-1 and 3A9. Elevated LFA-1/ICAM-1 unbinding forces were observed in the cell-cell measurements when the cells were treated with Mg^{2+}/EGTA (Fig. 5 *B*). The overlaid force spectra of LFA-1/ICAM-1 interaction acquired using resting 3A9 cells (Fig. 5 *C*) or Mg^{2+}/EGTA-activated cells (Fig. 5 *D*) and immobilized or cell-bound ICAM-1 are given in Fig. 5.

In our AFM measurements it was assumed that the measured rupture force stemmed from the unbinding of the LFA-1/ICAM-1 complex, although there are other linkages that can break during the force measurement. For example, it is conceivable that (1) ICAM-1 become unbound from the surface of the petri dish or that (2) LFA-1 is extracted from the cell membrane. We have carried out experiments to rule out these two possibilities. To demonstrate that LFA-1

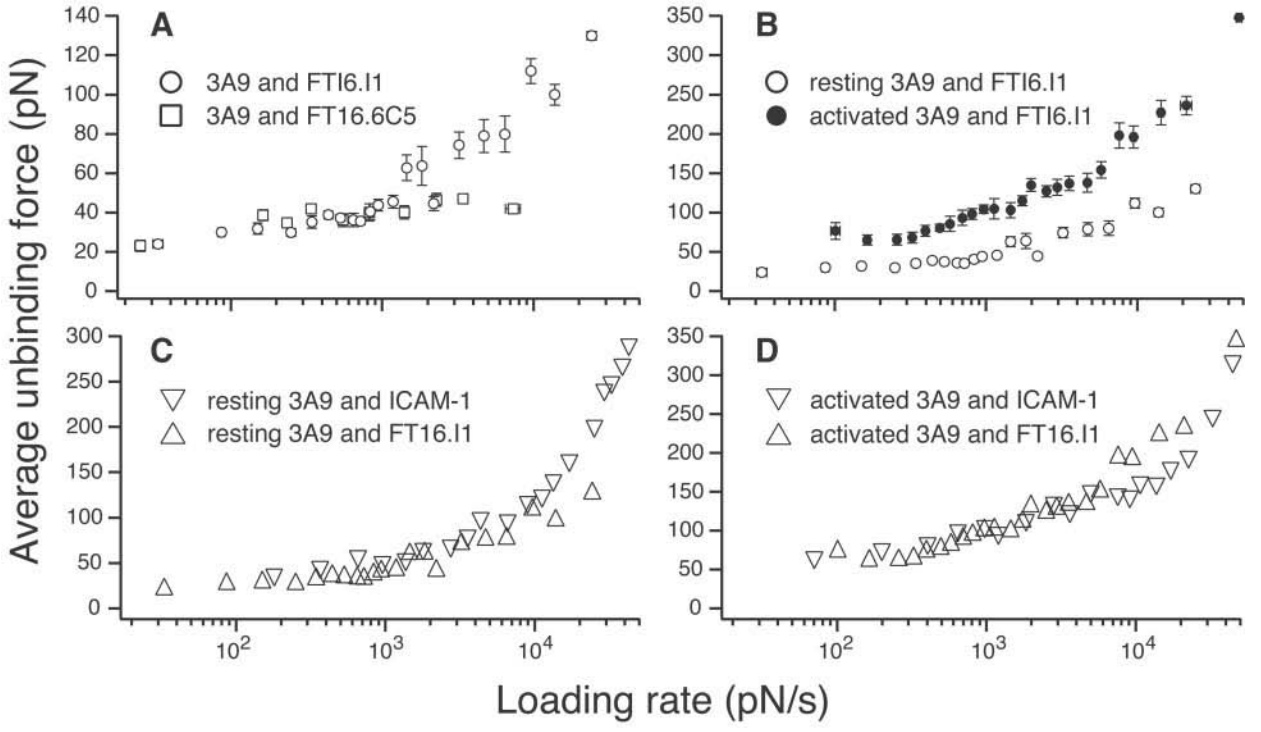

FIGURE 5 Measurements of individual LFA-1/ICAM-1 unbinding force between 3A9 cells and membrane bound ICAM-1. (*A*) Measurements between untreated 3A9 cells and the ICAM-1 expressing cell line FT16.I1 (*circles*) or the ICAM-1 negative cell line FT16.6C5 (*squares*). (*B*) Measurements between 3A9 cells and FT16.I1 in the absence (*open circles*) and presence (*filled circles*) of Mg^{2+}/EGTA. (*C*) Superimposed measurements of interactions between resting 3A9 cells and iICAM-1 (*inverted triangles*), and between resting 3A9 and FT16.I1 (*triangles*). (*D*) Superimposed measurements of interactions between Mg^{2+} -activated 3A9 cells and iICAM-1 (*inverted triangles*), and between activated 3A9 and FT16.I1 (*triangles*). Each of the force spectra was acquired using five cells with an average of 100 measurements/cell. The error bars are the standard error of the measurements.

remained anchored to the cell membrane, we acquired force measurements from Mg^{2+}-stimulated 3A9 cells that were fixed by a brief exposure to a 1% glutaraldehyde solution. As shown in Fig. 6, the force spectrum of the high-affinity LFA-1/ICAM-1 complex obtained using the fixed cells is similar to the force spectrum obtained using live cells. Since glutaraldehyde cross-linked LFA-1 with other membrane proteins and with components of the cytoskeleton, this result demonstrates that LFA-1 remained attached to the cell during the force measurements. Similarly, it is unlikely that the breakage occurred at the ICAM-1/substrate linkage. We have acquired overlapping force spectra of the LFA-1/ICAM-1 interaction with ICAM-1 bound to the petri dish and ICAM-1 expressed on the surface of FT16.I1 cells (Fig. 5). If breakage were to occur at the ICAM-1/substrate linkage, it is unlikely that the acquired force spectra would overlap. It should be noted that our experiments directly pointed to a breakage at LFA-1/ICAM-1 linkage. The force measurements revealed that the strength of the measured linkage was enhanced by Mg^{2+} or Mn^{2+}, but not by Ca^{2+}. It is well established that the LFA-1 is activated by Mg^{2+} and Mn^{2+}, but not by Ca^{2+} (Ganpule et al., 1997; Stewart et al., 1996). Because it is unlikely that the LFA-1-cell linkage or the ICAM-1-substrate linkage would exhibit such divalent cation dependency, we conclude that the acquired force measurements corresponded to the rupture force of the LFA-1/ICAM-1 complex.

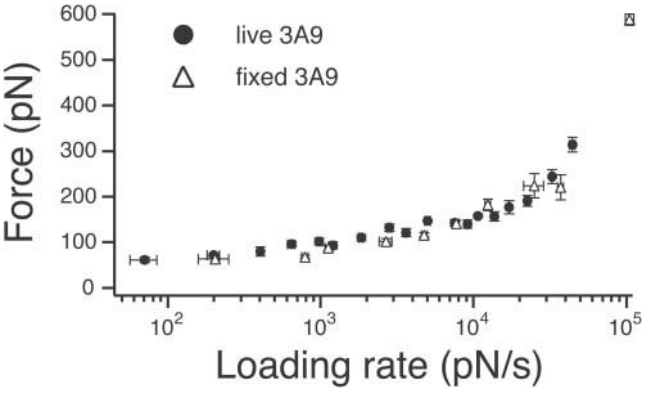

FIGURE 6 Measurements of the interactions between live 3A9 (*circles*) or fixed 3A9 cells (*triangles*) and iICAM-1 in Mg^{2+}/EGTA. The force spectrum of the untreated cell was derived from five cells and ~500 measurements. The force spectrum of the glutaraldehyde-fixed cell was derived from two cells and ~200 measurements. The error bars are the standard error of the measurements.

DISCUSSION

Beyond the observation that the mechanical strength of the high-affinity LFA-1/ICAM-1 complex is stronger than that of the low-affinity complex, the force spectra of the LFA-1/ICAM-1 interaction provided insight into the dissociation pathway of the complex. Our analysis of the unbinding of the LFA-1/ICAM-1 complex used the Bell model (Bell, 1978; Evans and Ritchie, 1997), which has been applied to studies of other ligand-receptor systems (Chen and Springer, 2001; Evans et al., 2001; Merkel et al., 1999). In the context of this model, a pulling force f distorts the energy landscape of the LFA-1/ICAM-1 complex, resulting in a lowering of the activation barrier(s), and consequently increases the dissociation rate constant $k(f)$ as follows: $k(f) = k^\circ \exp[f\gamma/k_BT]$, where k° is the dissociation rate constant in the absence of the pulling force, γ is the position of the transition state, T is temperature, and k_B is Boltzmann's constant. Under the conditions of constant loading r_f, the probability density function for the unbinding of a complex at force f is given by:

$$P(f) = k^\circ \exp\left(\frac{\gamma f}{k_BT}\right)\exp\left\{\frac{k^\circ k_BT}{\gamma r_f}\left(1 - \exp\left(\frac{\gamma f}{k_BT}\right)\right)\right\}. \quad (1)$$

Moreover, it can be shown that the average unbinding force of a complex, $\langle f_u \rangle$, increases with the rate of force application (i.e., loading rate), r_f, as follows:

$$\langle f_u \rangle = \frac{k_BT}{\gamma}\exp\left(\frac{k^\circ k_BT}{\gamma r_f}\right) E_1\left(\frac{k^\circ k_BT}{\gamma r_f}\right), \quad (2)$$

where $E_1(z)$ is the exponential integral, $E_1(z) = \int_1^\infty \exp(-zt)/t\,dt$ (Gergely et al., 2000; Tees et al., 2001b).

Equation 2 describes the dynamic properties of a system consisting of a single activation barrier. In cases where the dissociation process involves multiple transition states, a pulling force can suppress the outer activation barrier(s), allowing one of the inner activation barriers to determine the dissociation rate. In this situation, the model predicts multiple regimes of loading, each characterized by the properties of the different activation barriers (Evans and Ritchie, 1997). Initial attempts at fitting the one transition state model to the LFA-1/ICAM-1 force spectra revealed that our measurements are inconsistent with this model. However, our measurements are compatible with a model that involves two activation energy barriers. The outer energy barrier was characterized by measurements obtained at the slow loading regime of 20 to 10,000 pN/s. At loading rates >10,000 pN/s the outer activation barrier was suppressed, making the inner activation barrier assessable. Table 1 lists the Bell model parameters, k° and γ, of the two energy barriers that were derived from fitting Eq. 2 to the experimental data using a nonlinear least-square analysis routine in Mathematica (Wolfram Research, Inc., Champaign, IL).

TABLE 1 Bell model parameters of the LFA-1/ICAM-1 interaction

LFA-1/ICAM-1 Pair	Loading Rate (pN/s)	k° (s^{-1})	γ (Å)
ILFA-1/iICAM-1	20–10,000	4	1.5
	10,000–50,000	57	0.18
hLFA-1/iICAM-1	20–10,000	0.17	2.1
	10,000–50,000	40	0.24
ILFA-1/iICAM-1 w/EDTA	20–50,000	1.6	2.8

The fitted curves are overlaid on the measurements presented in Fig. 4 *A*.

The force measurements provided a glimpse of the complex process of ligand-receptor unbinding. As discussed, our measurements revealed two activation barriers in the dissociation of the LFA-1/ICAM-1 complex (Fig. 7). Each of these activation barriers (i.e., TS_1 and TS_2) is characterized by two parameters: a dissociation rate constant, k_i°, and the position of the transition state, γ_i, where $i = 1$ refers to the inner activation barrier and $i = 2$ refers to the outer activation barrier of the complex. Because the transition over the outer barrier is the rate-limiting step in the dissociation of the unstressed complex, k_2° of the outer barrier should be comparable to the dissociation rate constant measured by conventional methods. Indeed, k_2° for the forced dissociation of the low-affinity LFA-1 (1LFA-1)/ICAM-1 complex (4 s^{-1}) is in good agreement with the dissociation rate constant of the low-affinity closed I-domain/ICAM-1 interaction (2.84 s^{-1}) measured by surface plasmon resonance experiments (Shimaoka et al., 2001). k_2° for the forced dissociation of high-affinity LFA-1 (hLFA-1) and ICAM-1

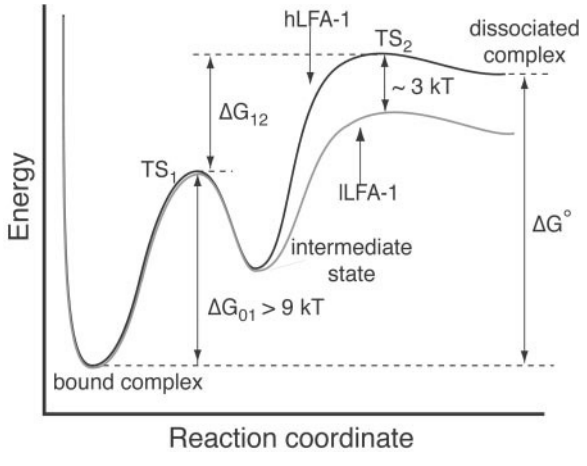

FIGURE 7 Intermolecular potentials of the murine LFA-1/ICAM-1 interaction. The dissociation of ICAM-1 from both high-affinity LFA-1 (hLFA-1) and low-affinity LFA-1 (1LFA-1) involves two transition states, TS_1 and TS_2. The inner activation barriers of the high and low-affinity complexes are >9 k_BT. Differences between the high and low-affinity complexes (~3 k_BT) stemmed from the energetics of the outer barriers. Estimates of the energies of transition states were obtained from the dissociation rate constants tabulated in Table 1. The positions of TS_1 and TS_2 were not drawn to scale.

($0.17\ s^{-1}$) is significantly slower than k_2° of the low-affinity interaction, but slightly faster than the reported dissociation rates of the high-affinity LFA-1/ICAM-1 interaction ($\sim 0.1\ s^{-1}$) (Lupher et al., 2001; Tominaga et al., 1998).

The dissociation rate constants were used to estimate the energy differences ($\Delta\Delta G^\dagger$) between transition state energies of high- and low-affinity complexes ($\Delta G_H^\dagger$ and $\Delta G_L^\dagger$): $\Delta\Delta G^\dagger = \Delta G_H^\dagger - \Delta G_L^\dagger = -k_BT \ln(k_H^\circ/k_L^\circ)$, where k_H° and k_L° are the dissociation rate constants of the high-and low-affinity complexes, respectively. This analysis revealed that the outer activation barrier of the high-affinity complex is 3.2 k_BT higher than that of the low-affinity complex. Moreover, our analysis revealed that the $\Delta\Delta G^\dagger$ of the inner barrier is small ($\sim 0.35\ k_BT$), which implies that the difference in equilibrium dissociation constant between the high- and low-affinity complexes stemmed from differences in the energies of the outer barrier.

The dissociation rate constants obtained from the force measurements can also be applied to estimate the transition state energies (Fig. 7). The energy between the transition states, TS_1 and TS_2, is given by $\Delta G_{12} = -k_BT \ln(k_2^\circ/k_1^\circ)$. ΔG_{12} of the low-affinity and high-affinity complexes are 2.7 and 5.5 k_BT, respectively. A lower limit for the activation energy of the inner barrier ΔG_{TS1} is the difference between the ΔG° and ΔG_{12}, where $\Delta G^\circ = -k_BT \ln K_d$. Taking the K_d values from Lollo et al. (1993), the corresponding ΔG° for the low- and high-affinity interaction is 9.2 and 14.8 k_BT, respectively. Hence, the lower limits for ΔG_{TS1} of the low-affinity and high-affinity complexes are 6.5 and 9.3 k_BT, respectively. Based on the observation that k° of the inner barrier is the same for high- and low-affinity complexes, we can conclude that ΔG_{TS1} of the low-affinity and high-affinity complexes are equal, and hence $>9.3\ k_BT$. Comparison of ΔG_{TS1} and ΔG_{12} further revealed that ΔG_{TS1} is $>77\%$ of the outer rate-determining activation energy barrier of the low-affinity complex, and at least 60% of the outer barrier of the high-affinity complex. This is significant because the position of the transition state of the inner barrier is ~ 0.2 Å from the bound state, and hence the inner barrier is very steep when compared to the outer barrier, which has its transition state 1.5–2 Å away.

At this time we cannot definitively assign structural elements to the two activation energy barriers. However, it is reasonable to assume that the inner activation energy stemmed from the ionic interaction between Glu-34 of ICAM-1 and the chelated Mg^{2+} of the α_L I domain. This view is supported by our measurements, which revealed that the presence of EDTA suppressed the unbinding force in the fast-loading regime, a region of the force spectrum that characterizes the inner activation energy of the complex. An interpretation of this result is that the chelated Mg^{2+} in the α_L I domain is transferred to EDTA, and thus cancels the ionic interaction between Glu-34 of ICAM-1 and MIDAS of the α_L I domain. The observation that EDTA did not alter the dynamic response of the complex in the slow-loading regime suggests that Mg^{2+} is not involved in the formation of the outer activation barrier. We propose that changes in the outer energy barrier that occurred following LFA-1 activation by Mg^{2+} originate from the predicted displacement of the $\alpha 7$ helix of the I domain (Leitinger and Hogg, 2000; Shimaoka et al., 2001). The resulting conformational change may expose a cryptic binding site and/or align the apposing molecular groups of LFA-1 and ICAM-1 for optimal interaction.

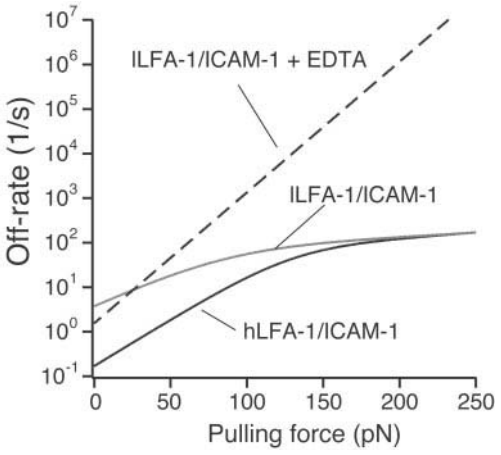

FIGURE 8 Kinetic profiles for rate of LFA-1 dissociation from ICAM-1 for high-affinity LFA-1, low-affinity LFA-1, and LFA-1 in the presence of 5 mM EDTA.

The consequences of the two activation energy barriers on the dynamic properties of the LFA-1/ICAM-1 complex are best illustrated in the kinetic profile of the complex (Fig. 8). The off-rate of the LFA-1/ICAM-1 complex in a two barrier model is given by:

$$k_{off} = 1/\{k_1^{\circ -1} \exp[-f\gamma_1/k_BT] + k_2^{\circ -1} \times \exp[-f\gamma_2/k_BT]\},$$

where indices in the subscript of the Bell model parameters refer to the inner and outer barriers (Evans et al., 2001). As shown in Fig. 8, the off-rate of the complex increases exponentially with pulling force. In both high- and low-affinity systems, there is initially a fast exponential raise in off-rate with applied force, followed by a more gradual exponential increase at forces $>\sim 150$ pN. In the high-force regime, the dissociation kinetics of both high- and low-affinity systems are nearly identical and are determined by the steep inner activation barrier. As a result of this steep inner barrier, the off-rate is less responsive to increases in pulling force. This point is highlighted when comparing the kinetic profiles of the LFA-1/ICAM-1 complex with and without EDTA. As discussed, the presence of EDTA suppressed the inner barrier of the complex, but left the outer barrier unaffected. In the absence of an inner steep barrier, the dissociation of the LFA-1/ICAM-1 complex is determined entirely by the outer activation energy barrier. Thus,

as illustrated in Fig. 8, the off-rate of the complex in the presence of EDTA is a simple exponential function of the pulling force. The major difference in the kinetic response of the LFA-1/ICAM-1 complex with and without EDTA occurred at high forces (i.e., >150 pN), where the off-rate of the complex with EDTA present is significantly faster than the off-rate of the complex in the absence of EDTA.

In summary, we propose that the dissociation of the LFA-1/ICAM-1 complex involves overcoming two activation barriers. The inner steep barrier allows the complex to resist large pulling forces and is attributed to the ionic interaction between Glu-34 of ICAM-1 and the I domain of LFA-1. Apparently, Mg^{2+} remains bound to the MIDAS of the I domain even in the low-affinity form of LFA-1, as the activation energy of the inner barrier is the same for both low- and high-affinity forms of LFA-1 (Lu et al., 2001). The affinity state of the LFA-1/ICAM-1 interaction is determined by the height of the outer activation energy barrier, which also determines the dissociation kinetics of the complex in the low-force regime.

We thank A. Chen for insightful discussions and C. Freites for technical support.

This work was supported by grants from the American Cancer Society and National Institutes of Health Grant 1 R29 GM55611-01.

REFERENCES

Bell, G. I. 1978. Models for the specific adhesion of cells to cells. *Science.* 200:618–627.

Bella, J., P. R. Kolatkar, C. W. Marlor, J. M. Greve, and M. G. Rossmann. 1998. The structure of the two amino-terminal domains of human ICAM-1 suggests how it functions as a rhinovirus receptor and as an LFA-1 integrin ligand. *Proc. Natl. Acad. Sci. USA.* 95:4140–4145.

Benoit, M., D. Gabriel, G. Gerisch, and H. E. Gaub. 2000. Discrete interactions in cell adhesion measured by single-molecule force spectroscopy. *Nat. Cell Biol.* 2:313–317.

Binnig, G., C. F. Quate, and C. Gerber. 1986. Atomic force microscope. *Phys. Rev. Lett.* 56:930–933.

Chen, S., and T. A. Springer. 2001. Selectin receptor-ligand bonds: formation limited by shear rate and dissociation governed by the Bell model. *Proc. Natl. Acad. Sci. USA.* 98:950–995.

Diamond, M. S., and T. A. Springer. 1994. The dynamic regulation of integrin adhessiveness. *Curr. Biol.* 4:506–517.

Dustin, M. L., and T. A. Springer. 1991. Role of lymphocyte adhesion receptors in transient interactions and cell locomotion. *Annu. Rev. Immunol.* 9:27–66.

Edwards, C. P., K. L. Fisher, L. G. Presta, and S. C. Bodary. 1998. Mapping the intercellular adhesion molecule-1 and -2 binding site on the inserted domain of leukocyte function-associated antigen-1. *J. Biol. Chem.* 273:28937–28944.

Evans, E., A. Leung, D. Hammer, and S. Simon. 2001. Chemically distinct transition states govern rapid dissociation of single L-selectin bonds under force. *Proc. Natl. Acad. Sci. USA.* 98:3784–3789.

Evans, E., and K. Ritchie. 1997. Dynamic strength of molecular adhesion bonds. *Biophys. J.* 72:1541–1555.

Florin E. L., V. T. Moy, and H. E. Gaub. 1994. Adhesion forces between individual ligand-receptor pairs. *Science.* 264:415–417.

Ganpule, G., R. Knorr, J. M. Miller, C. P. Carron, and M. L. Dustin. 1997. Low affinity of cell surface lymphocyte function-associated antigen-1 (LFA-1) generates selectivity for cell-cell interactions. *J. Immunol.* 159:2685–2692.

Gergely, C., J. Voegel, P. Schaaf, B. Senger, M. Maaloum, J. K. Horber, and J. Hermmerle. 2000. Unbinding process of adsorbed proteins under external stress studied by atomic force microscopy spectroscopy. *Proc. Natl. Acad. Sci. USA.* 97:10802–10807.

Heinz, W. F., and J. H. Hoh. 1999. Spatially resolved force spectroscopy of biological surfaces using the atomic force microscope. *Trends Biotechnol.* 17:143–150.

Huang, C., and T. A. Springer. 1995. A binding interface on the I domain of lymphocyte function-associated antigen-1 (LFA-1) required for specific interaction with intercellular adhesion molecule 1 (ICAM-1). *J. Biol. Chem.* 270:19008–19016.

Hutter, J. L., and J. Bechhoefer. 1993. Calibration of atomic-force microscope tips. *Rev. Sci. Instrum.* 64:1868–1873.

Hynes, R. O. 1992. Integrins: versatility, modulation, and signaling in cell adhesion. *Cell.* 69:11–25.

Kuhlman, P., V. T. Moy, B. A. Lollo, and A. A. Brian. 1991. The accessory function of murine intercellular adhesion molecule-1 in T lymphocyte activation. Contributions of adhesion and co-activation. *J. Immunol.* 146:1773–1782.

Larson, R. S., A. L. Corbi, L. Berman, and T. Springer. 1989. Primary structure of the leukocyte function-associated molecule-1 alpha subunit: an integrin with an embedded domain defining a protein superfamily. *J. Cell Biol.* 108:703–712.

Lee, G. U., L. A. Chrisey, and R. J. Colton. 1994b. Direct measurement of the forces between complementary strands of DNA. *Science.* 266: 771–773.

Lee, G. U., D. A. Kidwell, and R. J. Colton. 1994a. Sensing discrete streptavidin-biotin interactions with AFM. *Langmuir.* 10:354–361.

Lee, J. O., P. Rieu, M. A. Arnaout, and R. Liddington. 1995. Crystal structure of the A domain from the alpha subunit of integrin CR3 (CD11b/CD18). *Cell.* 80:631–638.

Leitinger, B., and N. Hogg. 2000. From crystal clear ligand binding to designer I domains. *Nat. Struct. Biol.* 7:614–616.

Lollo, B. A., K. W. Chan, E. M. Hanson, V. T. Moy, and A. A. Brian. 1993. Direct evidence for two affinity states for lymphocyte function-associated antigen 1 on activated T cells. *J. Biol. Chem.* 268: 21693–21700.

Lu, C., M. Shimaoka, Q. Zang, J. Takagi, and T. A. Springer. 2001. Locking in alternate conformations of the integrin alpha L beta 2 I domain with disulfide bonds reveals functional relationships among integrin domains. *Proc. Natl. Acad. Sci. USA.* 98:2393–2398.

Lupher, M. L., Jr., E. A. Harris, C. R. Beals, L. M. Sui, R. C. Liddington, and D. E. Staunton. 2001. Cellular activation of leukocyte function-associated antigen-1 and its affinity are regulated at the I domain allosteric site. *J. Immunol.* 167:1431–1439.

Marlin, S. D., and T. A. Springer. 1987. Purified intercellular adhesion molecule-1 (ICAM-1) is a ligand for lymphocyte function-associated antigen 1 (LFA-1). *Cell.* 51:813–819.

Merkel, R., P. Nassoy, A. Leung, K. Ritchie, and E. Evans. 1999. Energy landscapes of receptor-ligand bonds explored with dynamic force spectroscopy. *Nature.* 397:50–53.

Oberhauser, A. F., P. E. Marszalek, H. P. Erickson, and J. M. Fernandez. 1998. The molecular elasticity of the extracellular matrix protein tenascin. *Nature.* 393:181–185.

Qu, A., and D. J. Leahy. 1995. Crystal structure of the I-domain from the CD11a/CD18 (LFA-1, alpha L beta 2) integrin. *Proc. Natl. Acad. Sci. USA.* 92:10277–10281.

Rief, M., M. Gautel, F. Oesterhelt, J. M. Fernandez, and H. E. Gaub. 1997a. Reversible unfolding of individual titin immunoglobulin domains by AFM. *Science.* 276:1109–1112.

Rief, M., F. Oesterhelt, B. Heymann, and H. E. Gaub. 1997b. Single molecule force spectroscopy on polysaccharides by atomic force microscopy. *Science.* 275:1295–1297.

Sanchez-Madrid, F., P. Simon, S. Thompson, and T. A. Springer. 1983. Mapping of antigenic and functional epitopes on the alpha- and beta-

subunits of two related mouse glycoproteins involved in cell interactions, LFA-1 and Mac-1. *J. Exp. Med.* 158:586–602.

Shimaoka, M., C. Lu, R. T. Palframan, U. H. von Andrian, A. McCormack, J. Takagi, and T. A. Springer. 2001. Reversibly locking a protein fold in an active conformation with a disulfide bond: integrin alpha L I domains with high affinity and antagonist activity in vivo. *Proc. Natl. Acad. Sci. USA.* 98:6009–6014.

Siu, G., S. M. Hedrick, and A. A. Brian. 1989. Isolation of the murine intercellular adhesion molecule 1 (ICAM-1). *J. Immunol.* 143: 3813–3820.

Springer, T. A. 1990. Adhesion receptors of the immune system. *Nature.* 346:425–434.

Springer, T. A. 1994. Traffic signals for lymphocyte recirculation and leukocyte emigration: the multistep paradigm. *Cell.* 76:301–314.

Springer, T. A. 1997. Folding of the N-terminal, ligand-binding region of integrin alpha-subunits into a beta-propeller domain. *Proc. Natl. Acad. Sci. USA.* 94:65–72.

Stanley, P., and N. Hogg. 1998. The I domain of integrin LFA-1 interacts with ICAM-1 domain 1 at residue Glu-34 but not Gln-73. *J. Biol. Chem.* 273:3358–3362.

Staunton, D. E., M. L. Dustin, H. P. Erickson, and T. A. Springer. 1990. The arrangement of the immunoglobulin-like domains of ICAM-1 and the binding sites for LFA-1 and rhinovirus. *Cell.* 61:243–254.

Stewart, M. P., C. Cabanas, and N. Hogg. 1996. T cell adhesion to intercellular adhesion molecule-1 (ICAM-1) is controlled by cell spreading and the activation of integrin LFA-1. *J. Immunol.* 156: 1810–1817.

Stewart, M., and N. Hogg. 1996. Regulation of leukocyte integrin function: affinity vs. avidity. *J. Cell Biochem.* 61:554–561.

Tees, D. F., R. E. Waugh, and D. A. Hammer. 2001a. A microcantilever device to assess the effect of force on the lifetime of selectin-carbohydrate bonds. *Biophys. J.* 80:668–682.

Tees, D. F. J., J. T. Woodward, and D. A. Hammer. 2001b. Reliability theory for receptor-ligand bond dissociation. *J. Chem. Phys.* 114: 7483–7496.

Tominaga, Y., Y. Kita, A. Satoh, S. Asai, K. Kato, K. Ishikawa, T. Horiuchi, and T. Takashi. 1998. Affinity and kinetic analysis of the molecular interaction of ICAM-1 and leukocyte function-associated antigen-1. *J. Immunol.* 161:4016–4022.

Willemsen, O. H., M. M. Snel, A. Cambi, J. Greve, B. G. de Grooth, and C. G. Figdor. 2000. Biomolecular interactions measured by atomic force microscopy. *Biophys. J.* 79:3267–3281.

Woska, J. R., Jr., M. M. Morelock, D. D. Jeanfavre, and B. J. Bormann. 1996. Characterization of molecular interactions between intercellular adhesion molecule-1 and leukocyte function-associated antigen-1. *J. Immunol.* 156:4680–4685.